

Communication

Preparation and Cycling Performance of Iron or Iron Oxide Containing Amorphous Al-Li Alloys as Electrodes

Franziska Thoss ^{1,2,*}, Lars Giebeler ^{1,2}, Karsten Weißer ^{1,3}, Jörg Feller ³ and Jürgen Eckert ^{1,2}

¹ Leibniz Institute for Solid State and Materials Research Dresden (IFW), Institute for Complex Materials, Helmholtzstr. 20, D-01069 Dresden, Germany; E-Mails: l.giebeler@ifw-dresden.de (L.G.); karsten_weisser@gmx.de (K.W.); j.eckert@ifw-dresden.de (J.E.)

² Institute of Materials Science, Technische Universität Dresden, Helmholtzstr. 7, D-01069 Dresden, Germany

³ Hochschule für Technik und Wirtschaft Dresden, Faculty of Mechanical Engineering/Process Engineering, Friedrich-List-Platz 1, D-01069 Dresden, Germany; E-Mail: feller@mw.htw-dresden.de

* Author to whom correspondence should be addressed; E-Mail: f.thoss@ifw-dresden.de; Tel.: +49-351-4659694; Fax: +49-351-4659452.

External Editor: Duncan Gregory

Received: 23 September 2014; in revised form: 3 November 2014 / Accepted: 4 December 2014 / Published: 12 December 2014

Abstract: Crystalline phase transitions cause volume changes, which entails a fast destroying of the electrode. Non-crystalline states may avoid this circumstance. Herein we present structural and electrochemical investigations of pre-lithiated, amorphous Al₃₉Li₄₃Fe₁₃Si₅-powders, to be used as electrode material for Li-ion batteries. Powders of master alloys with the compositions Al₃₉Li₄₃Fe₁₃Si₅ and Al₃₉Li₄₃Fe₁₃Si₅ + 5 mass-% FeO were prepared via ball milling and achieved amorphous/nanocrystalline states after 56 and 21.6 h, respectively. In contrast to their Li-free amorphous pendant Al₇₈Fe₁₃Si₉, both powders showed specific capacities of about 400 and 700 Ah/kg_{Al}, respectively, after the third cycle.

Keywords: Li-ion batteries; metallic anodes; amorphous; ball milling; iron oxide

1. Introduction

Inventing and engineering better electrode materials for batteries, especially for Li-ion batteries, is of high interest, particularly with regard to a reduction of the fuel consumption. In general, graphite is a reliable anode material, but limited by a specific capacity of 372 Ah/kg. To exceed this capacity to enlarge energy and power density strong effort is made to establish intermetallic anodes for application in Li-ion batteries (e.g., LiAl, $\text{Li}_{22}\text{Si}_{14}$) due to their high theoretic specific capacities reached by Li content-induced phase transitions. The crucial point is to prevent cracking of these brittle phases caused by (de)lithiation. To avoid crystal cracking amorphization of the primary materials is one of many imaginable approaches. From the metallurgical point of view addition of so-called glass forming elements (e.g., rare earth elements or transition metals) to reach an amorphous state is still necessary. Nevertheless, besides improving properties of materials by modifying microstructures it is desirable to apply environmentally acceptable and cheap materials and to prove, whether already known working mechanisms can be transferred. In case of the amorphous alloys $\text{Al}_{86}\text{Ni}_{18}\text{Y}_6$ and $\text{Al}_{43}\text{Li}_{43}\text{Ni}_{18}\text{Y}_6$ [1,2] it is useful to substitute the rare earth element Y and the health hazardous element Ni by alternative elements which serve the same purpose.

For this reason, a new Al-Li-based alloy, including Fe and Si instead of Y and Ni, was investigated. According to the Li-integration into $\text{Al}_{86}\text{Ni}_{18}\text{Y}_6$, resulting in the master alloy $\text{Al}_{43}\text{Li}_{43}\text{Ni}_{18}\text{Y}_6$ [2], here Li is metallurgically blended into the conventional amorphous alloy $\text{Al}_{78}\text{Fe}_{13}\text{Si}_9$, resulting in the new alloy $\text{Al}_{39}\text{Li}_{43}\text{Fe}_{13}\text{Si}_5$. As demonstrated [2] it is very important to provide Li already within the primary alloy, since otherwise the free volume of a Li-free amorphous network is too small to allow for a significant Li-insertion. Preparing such Li-containing amorphous alloys is not trivial because the conventional melt spinning process is not possible due to Li sprinkling. In addition, high energy ball milling presents some difficulties due the high plasticity of Li. For this work, ball milling was successful as the necessary parameters had been achieved. An advantage of this choice of elements is that besides Al also Si is able to form Li-containing phases electrochemically. As we observed in former studies, the milling of an $\text{Al}_{43}\text{Li}_{43}\text{Ni}_{18}\text{Y}_6$ alloy in a conventional steel vial leads to significant Fe wear debris, which partially contains Fe^{3+} . The powder prepared in this way yielded a higher specific capacity and a better cycling stability than the same powder milled in a non-abrasive silicon nitride vial. This may be caused by Fe-oxide, which can also react with Li [2] by means of conversion reactions.

Regarding the forming of amorphous alloys, the Al-Fe-Si system was extensively investigated, basically by melt spinning methods [3–6]. In contrast, researching of Fe as additional element for alloy anodes in Li-ion batteries was rarely done. In general, Fe is assumed to have a positive effect on the cycling behavior. For example, the addition of Fe enhanced the reversible capacity of a Si-N compound (from 50 mAh/g up to 200 mAh/g) [7] and of an Al-C composite (216 mAh/g up to 255 mAh/g) [8]. In principle, the effect was explained by the restraining of volumetric changes, caused by the presence of Al-Fe-phases. To our understanding, this thesis can only provide an explanation for a better reversibility, but not for a higher capacity. The electrochemical performance of the specific phase Fe_2Al_5 was tested with respect to the effect of milling time by Lindsay *et al.* [9]. With increased milling time, a higher initial specific capacity was achieved, perhaps caused by a reduced particle size, while cycling stability remained poor. Fleischauer *et al.*, investigated Si-Al-Fe thin-film libraries [10]. They reported that alloys with a transition metal content of 20–50 at.% do not alloy with Li, which

lowers the achievable capacity. Furthermore, they postulated that the sputtered composition is only active if the corresponding crystalline phase is active. A well-known application of Fe as Li-ion battery anode material, differing from metallic materials, is given by conversion mechanisms of Fe-oxides [11].

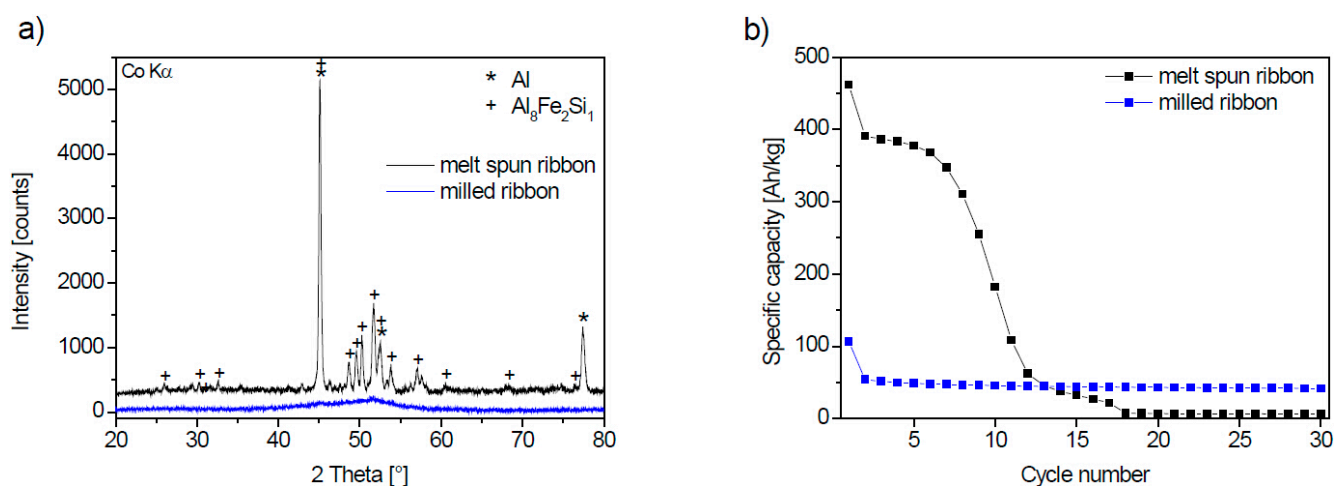
The herein presented experiments deal with elemental Fe as a component within the master alloy in order to substitute Ni as well as with FeO as an additive, which can in principle form Li-containing phases by means of conversion reactions.

Our work will help to answer the questions (i) if the mechanism of electrochemical cycling a Li-containing amorphous network as described in the system Al-Li-Ni-Y is transferable to the system Al-Li-Fe-Ni; and (ii) if conversion-like reactions play a role in this system.

2. Results and Discussion

On the basis of [12] und [13] ribbons of the alloy $\text{Al}_{78}\text{Fe}_{13}\text{Si}_9$ were prepared by melt spinning. With the parameters as per particulars given above, they did not turn to the amorphous state. Nevertheless, milling for 1.6 h led to the amorphous state (Figure 1a). Although this circumstance met the needed requirement and furthermore also had to be applied for the Li-containing alloy, the primary alloy system was not changed.

Figure 1. (a) XRD pattern; and (b) specific capacity during galvanostatic cycling at a charge rate of C/50 of melt spun and ball milled $\text{Al}_{78}\text{Fe}_{13}\text{Si}_9$ ribbons.



As expected from former studies [1], this amorphous alloy does not show a suitable specific capacity which is in agreement with the previously investigated alloy $\text{Al}_{86}\text{Ni}_{18}\text{Y}_6$ (Figure 1b and ref. [1]). For comparison, the specific capacity of the crystalline state is shown. Due to the volume changes and the contact losses it decreases rapidly.

Following these experiences with regard to the free volume, which is needed for lithiation [2], Li was added as component of the initial master alloy. That way, the alloy $\text{Al}_{39}\text{Li}_{43}\text{Fe}_{13}\text{Si}_5$ was pre-melted and afterwards ball milled in order to achieve an amorphous powder (Figure 2a). After 8 h the main phase LiAl has already diminished. After a milling time of 143.6 h, two relatively broad reflections remain, which differ from the observed phases of the initial alloy. Nevertheless, according to Lindsay *et al.*, these reflections could be assigned to an Al-Fe phase (Fe_2Al_3 or Fe_2Al_5 , respectively), possibly present as nanocrystals [9]. In any case, they do not have positions of LiAl reflections. After

milling, the powder has the chemical composition as shown in Table 1 (middle row). To conserve the global composition of the possibly inhomogeneous master alloy piece, no chemical analysis was done before milling.

Figure 2. (a) XRD-pattern of ball milled powders $\text{Al}_{39}\text{Li}_{43}\text{Fe}_{13}\text{Si}_5$; and (b) $\text{Al}_{39}\text{Li}_{43}\text{Fe}_{13}\text{Si}_5+\text{O}$.

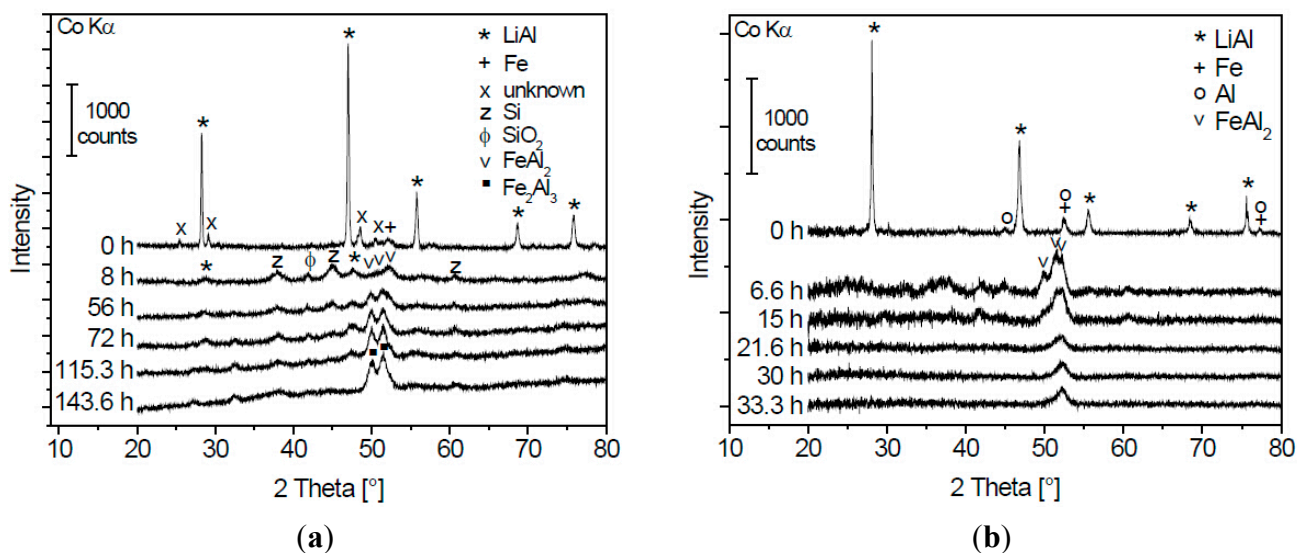


Table 1. Chemically analyzed composition (in at.%) of the samples $\text{Al}_{43}\text{Li}_{43}\text{Ni}_8\text{Y}_6^*$, $\text{Al}_{39}\text{Li}_{43}\text{Fe}_{13}\text{Si}_5$ and $\text{Al}_{39}\text{Li}_{43}\text{Fe}_{13}\text{Si}_5+\text{O}$.

Sample name	Al	Li	Ni	Y	Fe	Si	N/O**
$\text{Al}_{43}\text{Li}_{43}\text{Ni}_8\text{Y}_6^*$	21	26	4	2	6		41
$\text{Al}_{39}\text{Li}_{43}\text{Fe}_{13}\text{Si}_5$	33	34			8	4	17
$\text{Al}_{39}\text{Li}_{43}\text{Fe}_{13}\text{Si}_5+\text{O}$	22	26			4	2	46

* As published in [2], Fe is caused by wear debris. ** Referred to the average atomic mass of N and O, as almost equal and major parts of the non-metallic elements [2].

In contrast to the amorphous, Li-free pendant $\text{Al}_{78}\text{Fe}_{13}\text{Si}_9$ (Figure 1b) the sample $\text{Al}_{39}\text{Li}_{43}\text{Fe}_{13}\text{Si}_5$ can be lithiated reversibly and shows a significantly enhanced specific capacity of 500 Ah/kg_{Al} after the first cycle and 400 Ah/kg_{Al} after the third cycle (Figure 3). This functionalization is attained by pre-lithiation during the melting process. Even after the 30th cycle a capacity of about 300 Ah/kg_{Al} is observed in contrast to the same alloy-powder in its crystalline state (Figure 4). These results confirm that the process is in principle transferable to other alloys. Compared to the specific capacity of the previously investigated sample $\text{Al}_{43}\text{Li}_{43}\text{Ni}_8\text{Y}_6$ (composition in Table 1) the capacity of the sample $\text{Al}_{39}\text{Li}_{43}\text{Fe}_{13}\text{Si}_5$ is significantly lower (for better comparability referred to the Al-content). Capacities, assigned to content-specific weights, are displayed in Figure S1 in the electronic supplement. Melting and milling of $\text{Al}_{39}\text{Li}_{43}\text{Fe}_{13}\text{Si}_5$ was carried out as previously described for $\text{Al}_{43}\text{Li}_{43}\text{Ni}_8\text{Y}_6$ [2]. Non-metallic element contamination was much lower due to a redesigned valve. As a result, the atomic ratios of the other elements changed; in particular, the Al-content is significantly enhanced. This effect interferes with the only slightly enhanced Fe-content. Hence, a comparison of the two compositions is difficult, because the active mass besides the Al-content and the Si-content is unknown. For instance, Fe itself is unable to form any compounds with Li, but Fe-oxides and Fe-nitrides can participate in

electrochemical reactions according to the conversion mechanism [14,15]. However, O- and N-atoms solved in an amorphous network in combination with Fe-atoms might play a similar role.

Figure 3. Specific discharge capacity of the samples $\text{Al}_{43}\text{Li}_{43}\text{Ni}_8\text{Y}_6$ (with Fe wear debris, from ref. [2]), $\text{Al}_{39}\text{Li}_{43}\text{Fe}_{13}\text{Si}_5$ and $\text{Al}_{39}\text{Li}_{43}\text{Fe}_{13}\text{Si}_5+\text{O}$ during galvanostatic cycling at a charge rate of $C/50$. Different reference masses (referred to chemical analysis) are given in order to convey an impression. The alloys are difficult to compare because a change in the concentration of one component always causes a shift of the other atomic ratios.

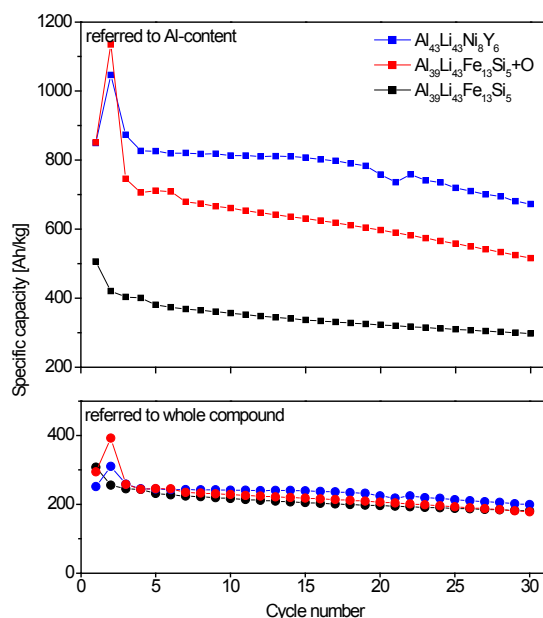
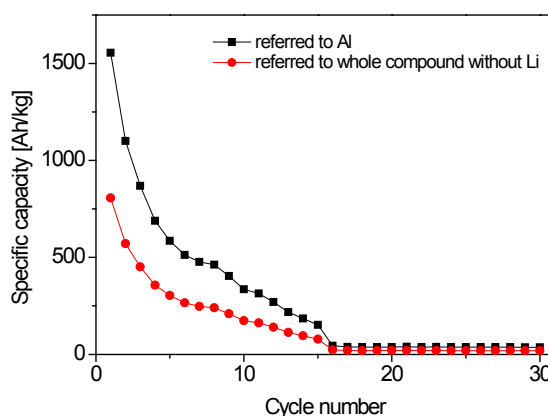


Figure 4. Specific discharge capacity of the crystallized sample $\text{Al}_{39}\text{Li}_{43}\text{Fe}_{13}\text{Si}_5$ during galvanostatic cycling at a charge rate of $C/50$.



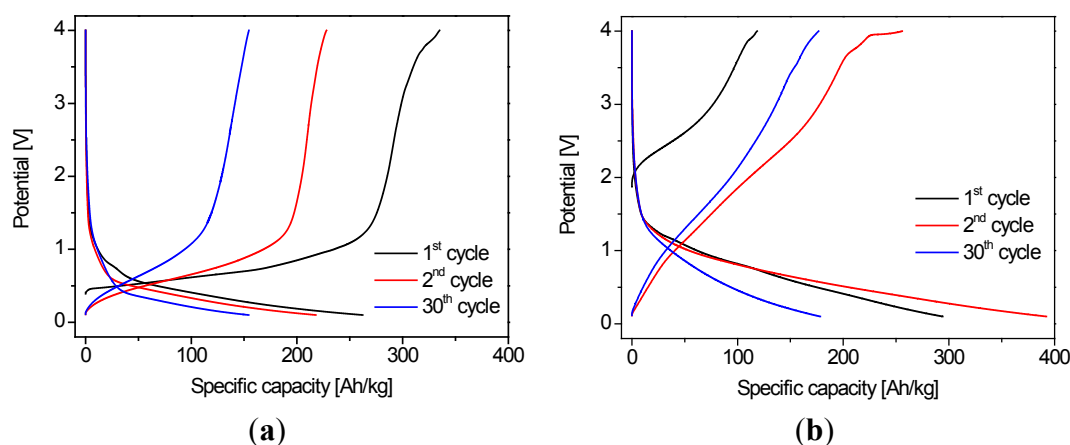
In order to achieve a comparable Al-content, the amount of the non-metallic elements was increased artificially by adding 5 wt.% FeO into the master alloy. The initial main phase LiAl disappears after a relatively short milling time (6.6 h), while the new phase FeAl_2 is formed. After 21.6 h the powder reaches a stable state indicated by an unchanged broad reflection in the X-ray pattern. According to the position of the reflection, FeAl_2 nanocrystals might be present (Figure 2b). The chemical composition after milling is documented in Table 1. The non-metallic content and the contents of Al and Li are in comparable ranges like for $\text{Al}_{43}\text{Li}_{43}\text{Ni}_8\text{Y}_6$.

As a result, the specific capacity was increased distinctly in comparison to the sample without additional FeO. The specific capacity is in the first cycle as high as observed for the sample $\text{Al}_{43}\text{Li}_{43}\text{Ni}_8\text{Y}_6$ and reaches a value of 850 Ah/kg (Figure 3). After the third cycle, the capacity is comparably lower and achieves 750 Ah/kg. Therefrom, non-metallic elements, solved in an amorphous network, may also contribute to the specific capacity.

Nevertheless, the following detail has to be noted: If the material contains high contents of non-metallic elements (as in $\text{Al}_{43}\text{Li}_{43}\text{Ni}_8\text{Y}_6$ and $\text{Al}_{39}\text{Li}_{43}\text{Fe}_{13}\text{Si}_5+\text{O}$), especially the delithiation potential window (charging) is very broad (Figure 5b). The profile (without faradaic plateau) is assumed to be connected with the diffusion process of Li into the amorphous network which may not correspond to a classical phase formation.

The alloy with a low nonmetal content ($\text{Al}_{39}\text{Li}_{43}\text{Fe}_{13}\text{Si}_5$) is delithiated and lithiated in a flat ramp at relatively low voltages between 0.1 and 1.2 V (Figure 5a). This property makes the material more suitable for an application as anode material.

Figure 5. (a) Delithiation and lithiation process of selected cycles of the samples $\text{Al}_{39}\text{Li}_{43}\text{Fe}_{13}\text{Si}_5$; and (b) $\text{Al}_{39}\text{Li}_{43}\text{Fe}_{13}\text{Si}_5+\text{O}$.



3. Experimental Section

Master alloys (compositions given in Table 1) were prepared by melting the pure elements Al (Alfa Aesar, Karlsruhe, Germany, 99.999%), Li (Alfa Aesar, Karlsruhe, Germany, 99.9%), Ni (Chempur, Karlsruhe, Germany, 99.98%), Y (Chempur, Karlsruhe, Germany, 99.9%), Fe (Chempur, Karlsruhe, Germany, 99.99%), Si (Chempur, Karlsruhe, Germany, 99.99%) and FeO (Alfa Aesar Karlsruhe, Germany, 99.5%; denoted as samples “+O”), respectively, within sealed Ta-tubes under Ar-atmosphere in an induction furnace (Trumpf Hüttinger, Freiburg, Germany). An ingot of the master alloy $\text{Al}_{78}\text{Fe}_{13}\text{Si}_9$ was melt-spun (E. Bühler D-7400, Hechingen, Germany) at 1200 °C through a quartz jet nozzle. The velocity of the rotating copper wheel was 30 m s⁻¹. High energy ball milling (Pulverisette 7 premium line, Fritsch, Idar-Oberstein, Germany) was carried out with steel milling vials equipped with pressure-relief valves. One milling cycle consisted of 10 min milling at 450 rpm and 20 min break. The milling times (without break) are 143.6 h ($\text{Al}_{78}\text{Fe}_{13}\text{Si}_9$), 48.5 h ($\text{Al}_{43}\text{Li}_{43}\text{Ni}_8\text{Y}_6$), 143.6 h ($\text{Al}_{39}\text{Li}_{43}\text{Fe}_{13}\text{Si}_5$) and 33.3 h ($\text{Al}_{39}\text{Li}_{43}\text{Fe}_{13}\text{Si}_5+\text{O}$), respectively. The powder compositions were chemically analyzed by inductively coupled plasma-optical emission spectrometry (ICP-OES, IRIS

Intrepid II, Thermo Fisher Scientific, Karlsruhe, Germany) of an alkaline fusion melt. X-ray powder diffraction was carried out by using a Panalytical Xpert Pro diffractometer with Co K α radiation and a Pixcel detector in Bragg-Brentano geometry. A part of the milled powder Al₃₉Li₄₃Fe₁₃Si₅ was annealed at 1000 °C under Ar-atmosphere in order to crystallize it completely. For electrochemical experiments, the powders were sieved in order to separate a fine particle fraction of 20–45 μ m in diameter. Subsequently, they were mixed with carbon (Super PLi, Timcal, Düsseldorf, Germany) and polyvinyliden difluoride (SOLEF 1013, Solvey, Hannover, Germany), as conductive and binding additives (ratio 8:1:1). Electrodes were prepared by pressing the mixtures onto steel grids (13 mm in diameter) and drying under Ar-atmosphere at 373 K for 12 h. The assembly of test cells (Swagelok, Berlin, Germany) was done in a glove box under O₂- and H₂O-controlled (<0.1 ppm) Ar-atmosphere using the electrolyte LP30 (1 M LiPF₆, 1:1 DMC/EC, Merck, Darmstadt, Germany) and lithium (Chemetall, Frankfurt, Germany, 99.9%) as counter electrode. The cells were electrochemically tested by galvanostatic cycling with a C-rate of C/50, related to elemental concentrations as found by chemical analysis.

4. Conclusions

The herein presented investigations show that harmful and rare elements like Ni and Y in their role as additive elements to help in the formation of amorphous alloys, can be replaced by Fe and Si also in Li-containing master alloys. As a result, the lithiation mechanism of the first investigated Li-containing amorphous Al-Li-Ni-Y system could successfully be transferred to another alloy. It was confirmed that the amorphous state is beneficial to avoid phase transitions, but Li has to be integrated metallurgically before electrochemical cycling. In combination with non-metallic elements like O and N, solved within the amorphous network, an enhancement of the specific capacity is observed. This behavior could be attributed to similar reactions as known from crystalline transition metal oxides and nitrides following the conversion mechanism. As a side effect, a significant broadening of the potential window for the delithiation/lithiation process is observed. In the present state, the material cannot be applied as industrial electrode material. From the academically point of view, a deeper understanding of mechanisms in combination with further investigations can lead to significant improvements in order to effectively manage this circumstance.

Acknowledgments

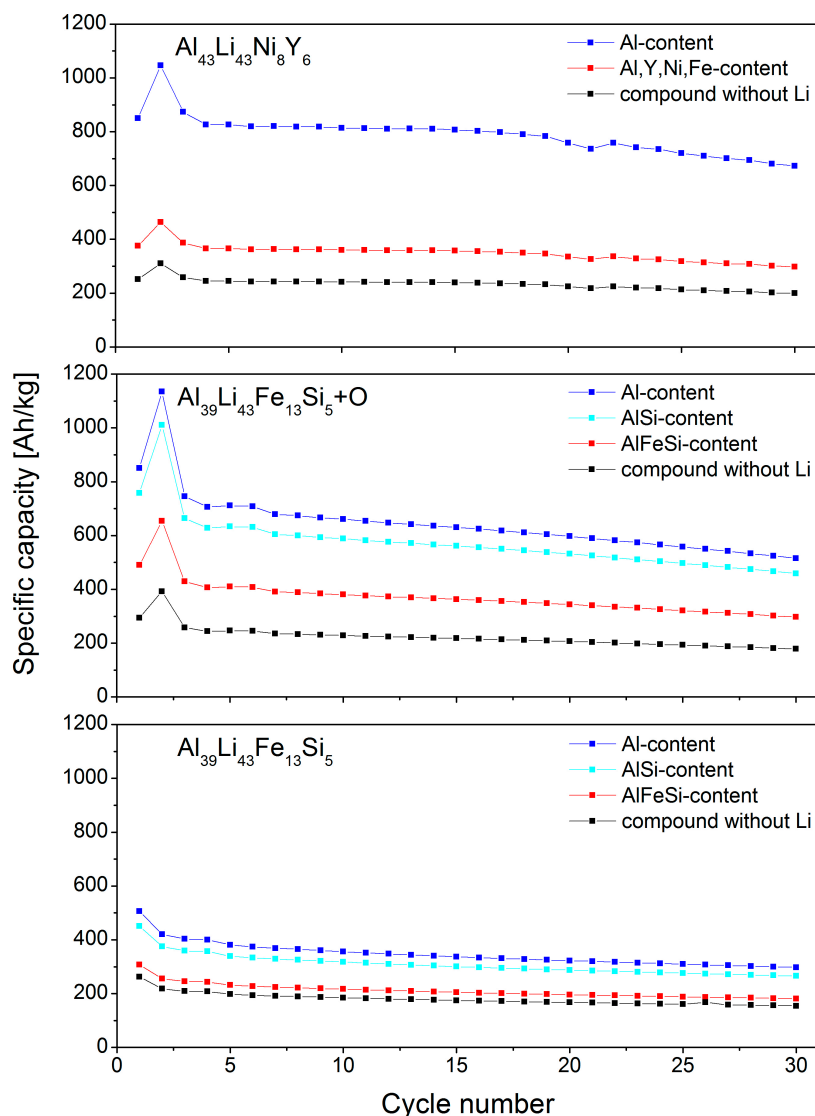
The authors are indebted to M. Frey and S. Donath for preparing the melt spun ribbons and A. Voss, A. Voidel and R. Buckan for carrying out the chemical analyses. F. Thoss gratefully acknowledges the Deutsche Bundesstiftung Umwelt (DBU) for financial funding. Further support was received from the Bundesministerium für Bildung und Forschung (BMBF) (Grant numbers 03X4637B and 03X4637C, Wing center – Excellent battery: Batterie - Mobil in Sachsen (BaMoSa)).

Author Contributions

F.T. conceived and designed the experiments; F.T. and K.W. performed the experiments and analyzed the data; F.T., L.G., J.F. and J.E. wrote the paper.

Appendix

Figure A1. Specific discharge capacities of the samples $\text{Al}_{43}\text{Li}_{43}\text{Ni}_8\text{Y}_6$ (with Fe wear debris, from ref. [2]), $\text{Al}_{39}\text{Li}_{43}\text{Fe}_{13}\text{Si}_5$ and $\text{Al}_{39}\text{Li}_{43}\text{Fe}_{13}\text{Si}_5+\text{O}$ during galvanostatic cycling at a charge rate of C/50. The different specific capacities are calculated with respect to the different element contents. For $\text{Al}_{39}\text{Li}_{43}\text{Fe}_{13}\text{Si}_5$ and $\text{Al}_{39}\text{Li}_{43}\text{Fe}_{13}\text{Si}_5+\text{O}$ an additional curve is given for the AlSi-content, because these both elements are electrochemically active in their crystalline states in contrast to Ni, Y and Fe.



Conflicts of Interest

The authors declare no conflict of interest.

References

1. Thoss, F.; Giebeler, L.; Oswald, S.; Ehrenberg, H.; Eckert, J. Study on the reversible Li-insertion of amorphous and partially crystalline $\text{Al}_{86}\text{Ni}_{18}\text{La}_6$ and $\text{Al}_{86}\text{Ni}_{18}\text{Y}_6$ alloys as anode materials for Li-ion batteries. *Electrochim. Acta* **2012**, *60*, 85–94.

2. Thoss, F.; Giebeler, L.; Thomas, J.; Oswald, S.; Potzger, K.; Reuther, H.; Ehrenberg, H.; Eckert, J. Amorphous Li-Al-based compounds: A novel approach for designing high performance electrode materials for Li-Ion batteries. *Inorganics* **2013**, *1*, 14–31.
3. Suzuki, R.O.; Komatsu, Y.; Kobayashi, K.F.; Shingu, P.H. Formation and crystallization of Al-Fe-Si amorphous alloys. *J. Mater. Sci.* **1983**, *18*, 1195–1201.
4. Dini, K.; Dunlap, R.A. The relationship of the quasicrystalline icosahedral phase to the amorphous structure in rapidly quenched Al-Mn-Si and Al-Fe-Si alloys. *J. Phys. F* **1986**, *16*, 1917–1925.
5. Bendersky, L.A.; Kaufman, M.J.; Boettinger, W.J.; Biancaniello, F.S. Solidification of an amorphous phase in rapidly solidified Al-Fe-Si alloys. *J. Mater. Sci. Eng.* **1988**, *98*, 213–216.
6. Inoue, A.; Bizen, Y.; Kimura, H.M.; Masumoto, T. Compositional range, thermal stability, hardness and electrical resistivity of amorphous alloys in Al-Si (or Ge) transition metal systems. *J. Mater. Sci.* **1988**, *23*, 3640–3647.
7. Doh, C.-H.; Kalaiselvi, N.; Park, C.-W.; Jin, B.S.; Moon, S.-I.; Yun, M.-S. Synthesis and electrochemical characterization of novel high capacity $\text{Si}_{3-x}\text{Fe}_x\text{N}_4$ anode for rechargeable lithium batteries. *Electrochem. Commun.* **2004**, *6*, 965–968.
8. Chen, Z.; Qian, J.; Ai, X.; Cao, Y.; Yang, H. Electrochemical performances of Al-based composites as anode materials for Li-ion batteries. *Electrochim. Acta* **2009**, *54*, 4118–4122.
9. Lindsay, M.J.; Wang, G.X. and Liu, H.K. Al-based anode materials for Li-ion batteries. *J. Power Sources* **2003**, *119–121*, 84–87.
10. Fleischauer, M.D.; Obrovac, M.N.; Dahn, J.R. Simple model for the capacity of amorphous silicon-aluminum-transition metal negative electrode materials. *J. Electrochem. Soc.* **2006**, *153*, A1201–A1205.
11. Li, J.; Li, J.; Luo, J.; Wang, L.; He, X. Recent Advances in the LiFeO_2 -based Materials for Li-ion Batteries. *Int. J. Electrochem. Sci.* **2011**, *6*, 1550–1561.
12. Srivastava, A.K.; Ranganathan, S. Microstructural characterization of rapidly solidified Al-Fe-Si, Al-V-Si, and Al-Fe-V-Si alloys. *J. Mater. Res.* **2001**, *16*, 2103–2117.
13. Schumacher, P.; Cizek, P. Heterogeneous nucleation mechanism in Al-Fe-Si amorphous alloys. *Mater. Sci. Eng. A* **2001**, *304–306*, 215–219.
14. Cabana, J.; Monconduit, L.; Larcher, D.; Palacín, M.R. Beyond intercalation-based Li-ion batteries: The state of the art and challenges of electrode materials reacting through conversion reactions. *Adv. Mater.* **2010**, *22*, E170–E192.
15. Marom, R.; Amalraj, S.F.; Leifer, N.; Jacob, D.; Aurbach, D. A review of advanced and practical lithium battery materials. *J. Mater. Chem.* **2011**, *21*, 9938–9954.